Supplement of Atmos. Meas. Tech., 12, 4543–4560, 2019
https://doi.org/10.5194/amt-12-4543-2019-supplement

Atmospheric Measurement Techniques
Open Access
EGU

Supplement of

Inter-comparison of elemental and organic carbon mass measurements from three North American national long-term monitoring networks at a co-located site

Tak W. Chan et al.

Correspondence to: Tak W. Chan (tak.chan@canada.ca) and Lin Huang (lin.huang@canada.ca)

Supplementary Material (12 pages, 2 table, and 6 figures):

Nomenclature

AIHL	Air-industrial hygiene laboratory
AMS	Accelerator mass spectrometry
BC	Black carbon
CABM	Canadian Aerosol Baseline Measurement
CAPMoN	Canadian Air and Precipitation Monitoring Network
CARE	Center for Atmospheric Research Experiment
CCMR	Climate Chemistry Measurements and Research
DRI	Desert Research Institute
DRI-TOR	CAPMoN measurements using IMPROVE on DRI analyzer with TOR correction
EC	Elemental carbon
ECCC	Environment and Climate Change Canada
ECT9	EnCan-Total-900 protocol
FID	Flame ionization detector
FLEXPART	FLEXible PARTicle dispersion model
ICP	Inter-comparison study
IMPROVE	Interagency Monitoring PROtected Visual Environments
IMPROVE_A TOR	IMPROVE_A TOR protocol on DRI analyzer
KCCAMS	Keck Carbon Cycle accelerator mass spectrometry
MAC	Mass absorption coefficient
NIST	National Institute of Standard and Technology
OC	Organic carbon
PM	Particulate matter
POC	Pyrolyzed organic carbon
PSAP	Particle Soot Absorption Photometer
SOA	Secondary organic aerosol
SRM	Standard Reference Material
Sunset-TOT	IMPROVE TOT protocol on Sunset analyzer
TC	Total carbon
TEA	Thermal evolution analysis
TOA	Thermal optical analysis
TOR	Thermal optical reflectance
TOT	Thermal optical transmittance
UCI	University of California Irvine
WMO	World Meteorological Organization

Thermal-Optical Analysis / Thermal Evolution Analysis

During the analysis of both thermal-optical analysis (TOA) and thermal evolution analysis (TEA), a small punch of the filter is placed either inside the Desert Research Institute (DRI) carbon analyzer (https://www.dri.edu/) or the Sunset laboratory-based carbon analyzer (http://www.sunlab.com) and subjected to a step-wise heating protocol.

IMPROVE_A (referred to as IMPROVE_A TOR in the manuscript) is a TOA protocol. The heating is in successive steps of 140°C (OC1), 280°C (OC2), 480°C (OC3), and 580°C (OC4) in helium (He) flow and 580°C (EC1), 740°C (EC2), and 840°C (EC3) in 2% O_2 and 98% He environment (Figure S1a; Table S1) (Chow et al, 2007). The evolved carbon is first oxidized to CO_2 then reduced to CH_4 and be determined by a flame ionization detector (FID). During the heating under a non-oxidative atmosphere, much of the OC will be combusted and leave the filter, some OC including the oxygenated compounds, char and turn to pyrolyzed organic carbon (POC) which would be combusted under an oxidative environment with EC. The POC mass defined in the IMPROVE_A TOR method is estimated by monitoring the reflectance (i.e., thermal optical reflectance; TOR) of a 633-650 nm laser beam within the oxidative environment. The combustion of POC result in an increased laser reflectance signal. When the reflectance signal returns to its initial intensity at the start of the analysis (i.e., prior to the formation of POC), it is assumed all POC is combusted and the remaining carbon mass in the analysis belongs to EC. The IMPROVE_A TOR protocol defines OC as OC1+OC2+OC3+OC4+POC while EC is defined as EC1+EC2+EC3-POC.

The IMPROVE (referred to as DRI-TOR in the manuscript) protocol is similar to the IMPROVE_A TOR protocol, and the heating steps in this TOA protocol includes 120°C (OC1), 250°C (OC2), 450°C (OC3), and 550°C (OC4) in He flow and 550°C (EC1), 700°C (EC2), and 800°C (EC3) in 2% O_2/98% He atmosphere (Figure S1b; Table S1) (Chow et al., 1993). OC is defined as OC1+OC2+OC3+OC4+POC while EC is defined as EC1+EC2+EC3-POC.

The EnCan-Total-900 (ECT9) is a TEA protocol that utilizes higher temperature set point and longer retention time (compared to DRI-TOR and IMPROVE_A TOR) for baseline separation of OC, POC, and EC (Huang et al., 2006; Chan et al., 2010). The ECT9 method consists of three temperature settings. First, two 600 s heating stages at 550°C and 870°C under pure He stream for OC and POC including carbonate carbon (CC) determination, respectively; then followed by EC determination over a 420 s heating at 900°C under 2% O_2 and 98% He atmosphere (Figure S1c; Table S1). Different from the DRI-TOR and IMPROVE_A TOR protocols, POC defined in ECT9 method is not a charring correction but represent different groups of organic compounds, as well as some calcium carbonate ($CaCO_3$) that does not combust under 550°C. The total OC in ECT9 method is defined as OC+POC.

Figure S1 Comparison of the (a) IMPROVE_A TOR, (b) DRI-TOR, and (c) EnCan-Total-900 (ECT9) protocols used in the different networks. Note that the time scale (i.e., x-axis scale) for DRI-TOR and IMPROVE_A TOR are for illustration purposes as both protocols are event driving depending on the particle loading on the filter punch.

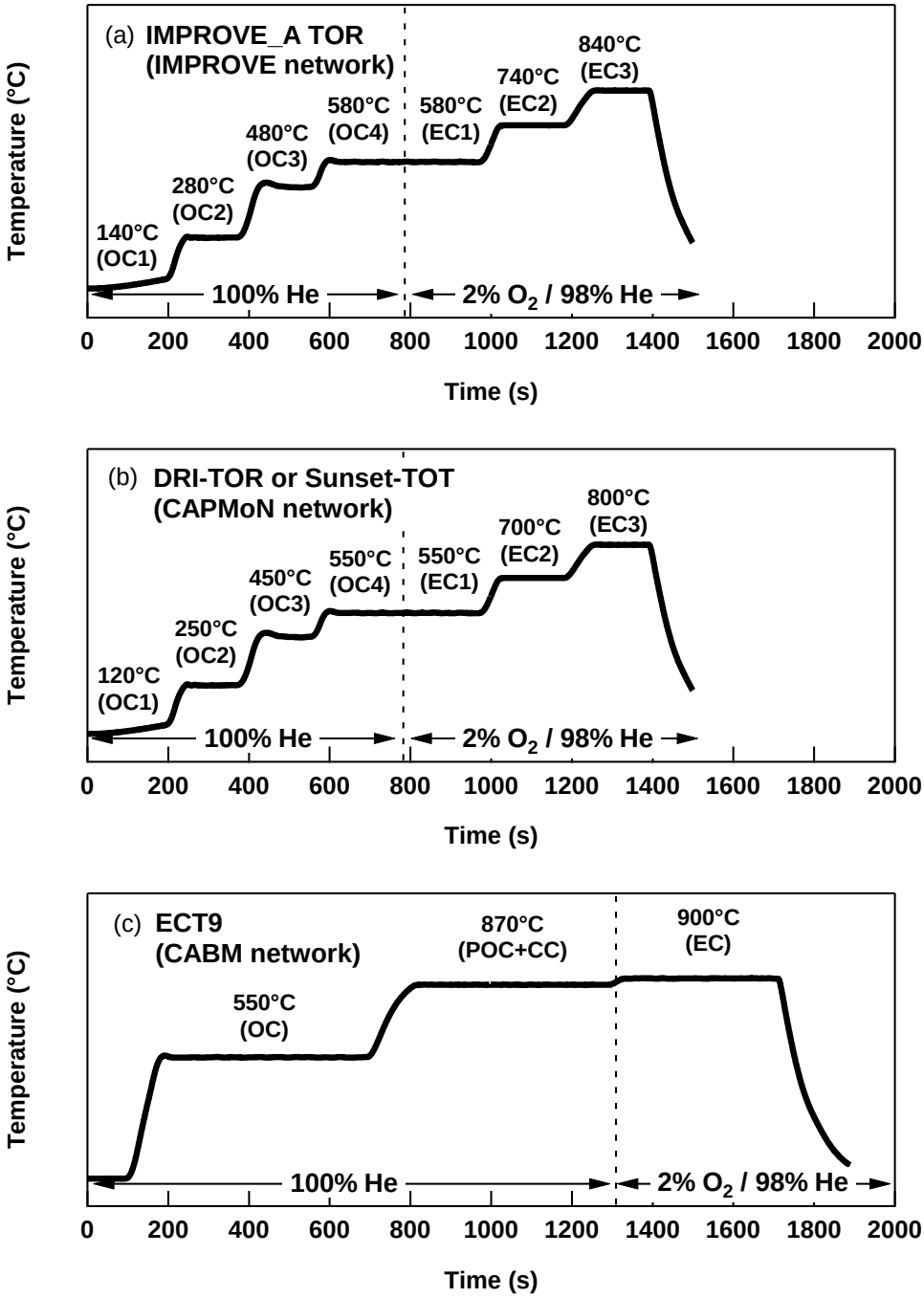

Table S1 Experimental parameters of the three TOA/TEA protocols used in this study.

Methods Carrier gas	Carbon fraction	IMPROVE_A TOR Temp (°C), Time (s)	DRI-TOR / Sunset-TOT Temp (°C), Time (s)	ECT9 Temp (°C), Time (s)
He-purge		30, 90	30, 90	90
He	OC1	140, 150-580	120, 150-600	-
He	OC2	280, 150-580	250, 150-600	-
He	OC3	480, 150-580	450, 150-600	-
He	OC4	580, 150-580	550, 150-600	-
He	OC	-	-	550, 600
He	POC	-	-	870, 600
O_2/He	EC1	580, 150-580	550, 150-600	-
O_2/He	EC2	740, 150-580	700, 150-600	-
O_2/He	EC3	840, 150-580	800, 150-600	-
O_2/He	EC	-	-	900, 420

Note: OC in IMPROVE_A TOR and DRI-TOR are defined as OC1+OC2+OC3+OC4+POC
EC in IMPROVE_A TOR and DRI-TOR are defined as EC1+EC2+EC3-POC
For ECT9, total OC is defined as OC+POC. For consistency purpose, the "ECT9 OC" discussed in this work refers to OC+POC.

Radiocarbon analysis

The $^{14}C/^{12}C$ abundances associated to the individual mass fractions of TC, OC and EC were determined using accelerator mass spectrometry (AMS) at the Keck Carbon Cycle AMS (KCCAMS) Facility at University of California Irvine (UCI). The KCCAMS/UCI runs an inhouse modified AMS compact instrument (0.5MV 1.5SDH-2) purchased from National Electrostatic Corporation (Beverly et al., 2010). Optimizations to the spectrometer couple with ultra-small sample capabilities (Santos et al., 2007) allowed for the measurement of single OC and/or EC fractions, besides TC samples. Mass fractions of TC, OC and EC isolated by the ECT9 protocol using a Sunset Laboratory instrument (Huang et al., 2006) was shipped to KCCAMS/UCI as cryogenically trapped CO_2 in sealed ampules followed by a separated set of reference materials. Isolated CO_2 samples were then converted to filamentous graphite following specific protocols (Santos and Xu, 2017) and analyzed for their carbon isotopes. Radiocarbon results as FM (fraction modern carbon) were corrected for background effects and isotopic fractionation with $\delta^{13}C$ of prepared graphite measured directly at the spectrometer, as described by Santos et al. (2007).

Figure S2 Box plots summarizing the magnitude of the gaseous adsorption, in (a) absolute value and (b) percentage, on CAPMoN TC, OC, POC, and EC mass measurements. Measurements prior to 2008 were obtained using the Sunset-TOT method while measurements from 2008-2015 were obtained using the DRI-TOR method. Each individual box represents the 25th, 50th, and 75th percentiles of the measurement values while the 10th and 90th percentiles are represented by the bottom and top whiskers, respectively.

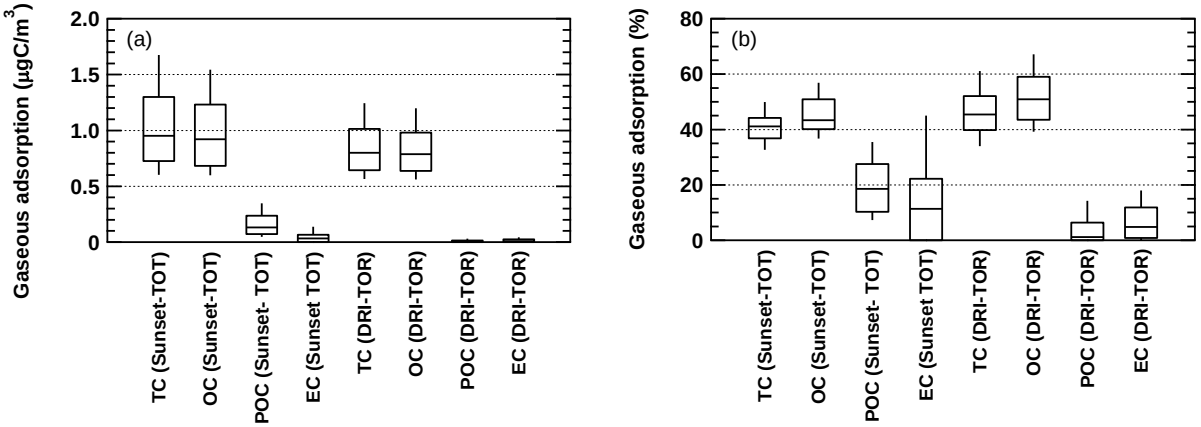

Figure S3 Monthly averaged ECT9 EC and IMPROVE_A TOR EC concentrations time series.

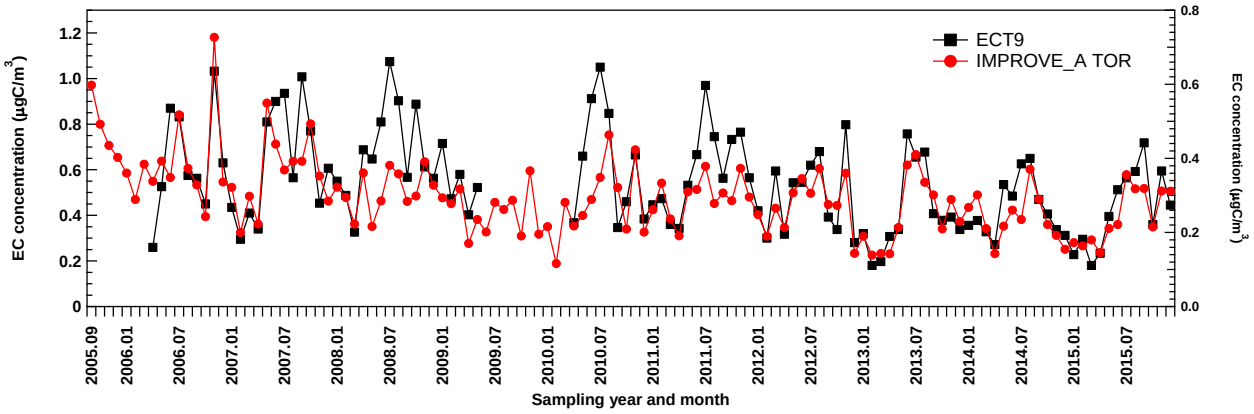

Table S2 Correlation coefficients (r) of various monthly averaged carbonaceous mass measurements among different networks (IMPROVE, CAPMoN and CABM). All measurements cover the period from 2008 to 2015.

		IMPROVE_A TOR				DRI-TOR				ECT9			
		TC	OC	EC	POC	TC	OC	EC	POC	TC	OC	EC	POC
IMPROVE_A TOR	TC	1	0.99	0.79	0.90	0.91	0.91	0.68	0.87	0.88	0.87	0.77	0.60
	OC		1	0.69	0.90	0.90	0.90	0.63	0.87	0.86	0.87	0.74	0.56
	EC			1	0.68	0.76	0.70	0.81	0.69	0.73	0.63	0.74	0.61
	POC				1	0.82	0.81	0.62	0.85	0.83	0.83	0.73	0.59
DRI-TOR	TC					1	0.99	0.74	0.92	0.79	0.78	0.71	0.41
	OC						1	0.63	0.92	0.77	0.77	0.67	0.40
	EC							1	0.63	0.63	0.56	0.69	0.31
	POC								1	0.77	0.75	0.70	0.44
ECT9	TC									1	0.98	0.91	0.70
	OC										1	0.82	0.75
	EC											1	0.50
	POC												1

Seasonality in Carbon Concentration and Possible Origination

To determine the air mass origins, a Lagrangian particle dispersion transport model (FLEXible PARTicle dispersion model; FLEXPART) (Stohl et al., 2005) was applied to obtain daily five-day back-trajectories from Egbert from 2006 to 2015. Figure S6 summarizes the average FLEXPART footprints for summer (May-Oct) and winter (Nov-Apr) seasons, showing the probability of air masses originating from various regions. These results indicate regional contributions from boreal forest in the northern part of Ontario and Quebec, as well as anthropogenic emissions from the northern U.S. Five-day trajectories show larger concentrations from the N and NW, consistent with wind roses shown in Figure S4.

At low ambient temperatures, primary emissions (e.g., local transportation, residential heating, and industrial activities) account for most of the ambient OC and EC (Ding et al., 2014). Increased human activities (e.g., traveling by car and barbecuing) during warmer weather could lead to increased emissions. High ambient temperature also leads to increased biogenic emissions (e.g., monoterpenes) from the boreal forest and increased SOA formation (Chan et al., 2010; Leaitch et al., 2011; Passonen et al., 2013; Tunved et al., 2006). The central and eastern boreal forest fire season typically occurs from May to August when ambient air is dry and hot, resulting in generally increased OC and EC emissions (Lavoué et al 2000). Transboundary transport of biomass burning emissions from the U.S. could also contribute to the higher concentrations in southern Ontario (Healy et al. 2017). Increasing ambient temperature from 10 °C to 20 °C leads to higher OC concentrations from 0.84 to 1.61 $\mu gC/m^3$ (91.7% increase) and EC concentration from 0.31 to 0.45 $\mu gC/m^3$ (45.2% increase). The temperature dependency of OC and EC suggests a potential climate feedback mechanism consistent with the observations from Leaitch at al. (2011) and Passonen et al. (2013).

Figure S4 Wind rose analysis (by month) based on the local wind speed and direction data for various months obtained at Egbert over the period from 2006 to 2015.

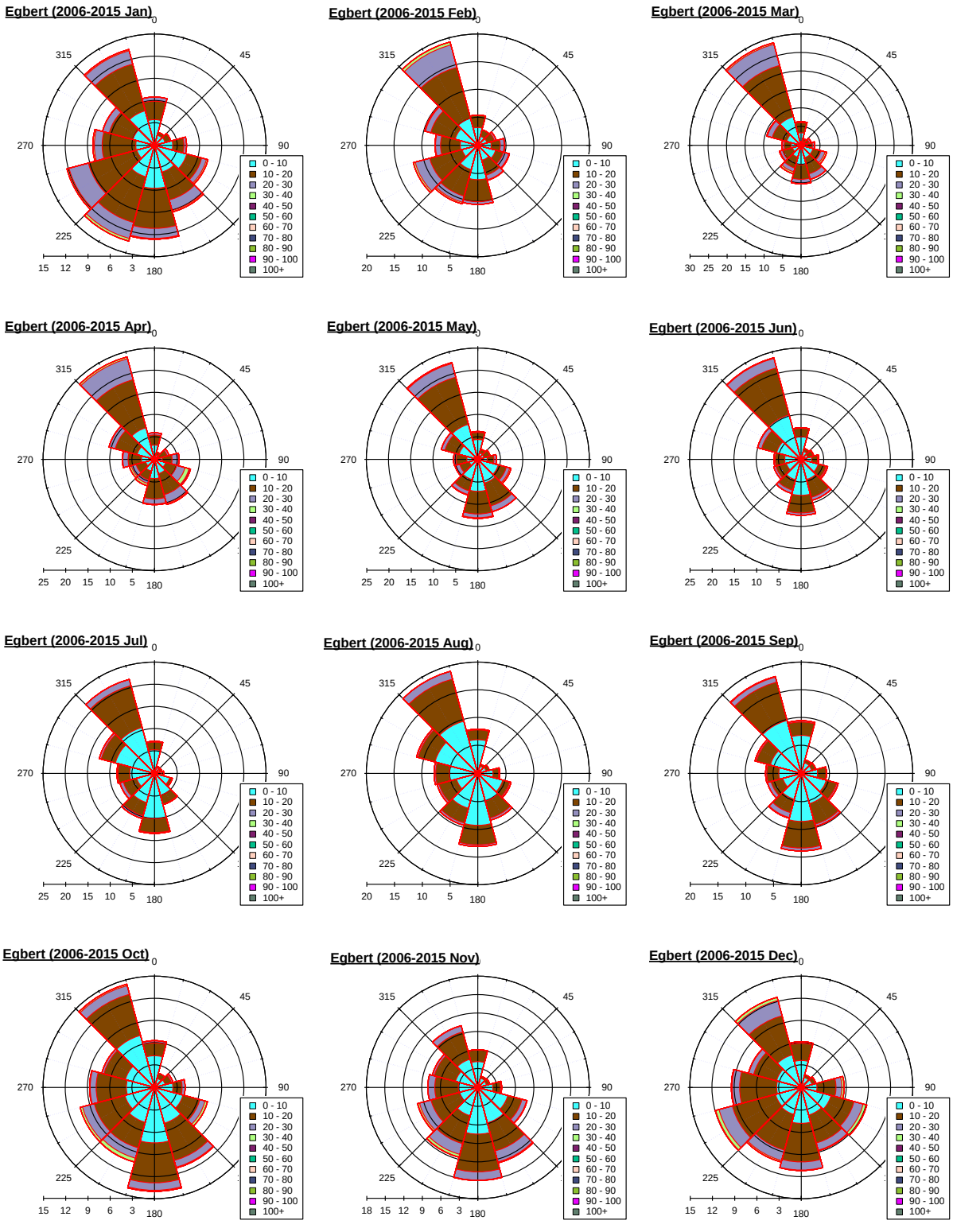

Figure S5 Figure shows the relationship of (a) TC, (b) OC, and (c) EC as a function of ambient temperature. IMPROVE, CAPMoN, and CABM measurements are represented by the black, orange, and blue markers, respectively. The red trace represents the best-fitted Sigmoid function on all measurement while the red dashed lines cover the 95% confidence interval of the best-fit function.

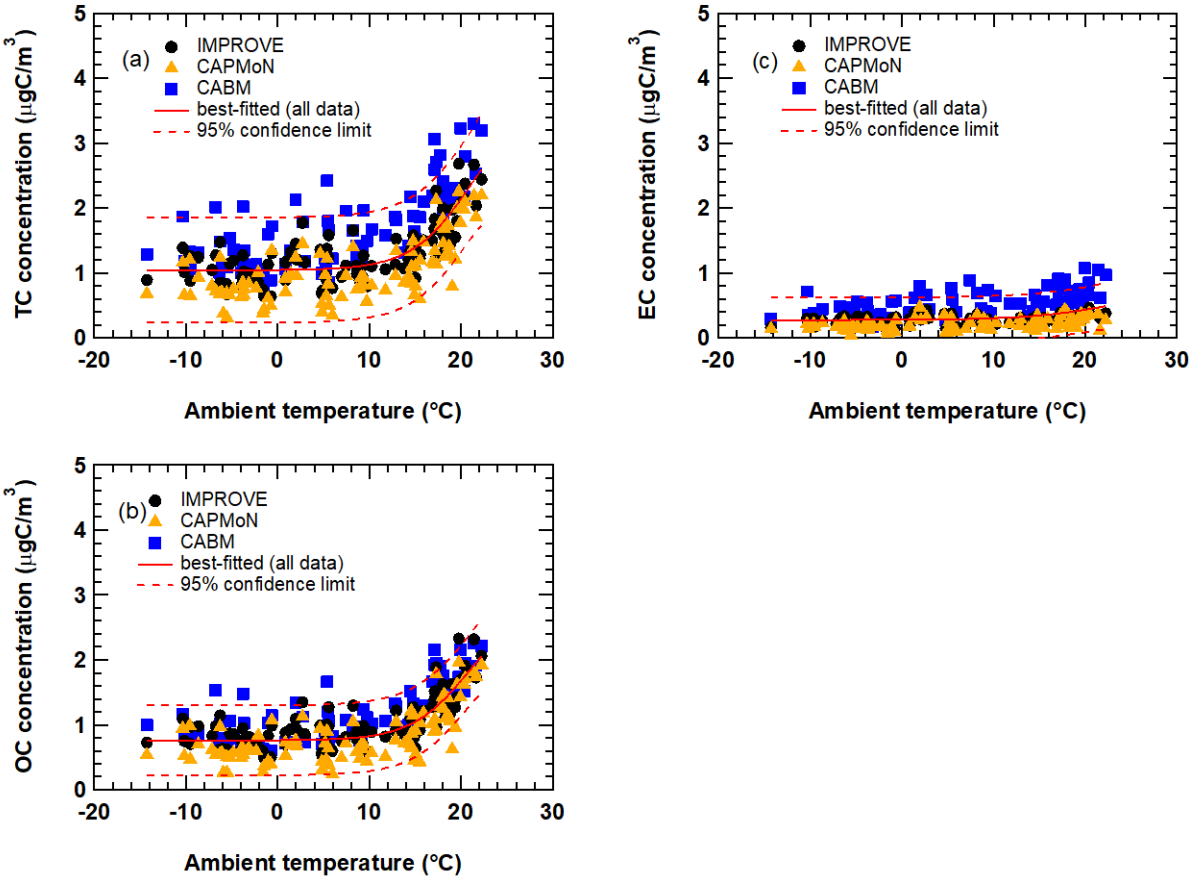

Figure S6 Figure showing the average air masses footprint reaching Egbert derived from FLEXPART. Results are derived from daily footprint over the period from 2006 to 2015, from (a) May to October and (b) November to April. Red, green, and purple colors represent the relative probability of the air masses origin in decreasing likelihood. To improve the visibility, results are plotted on log scale.

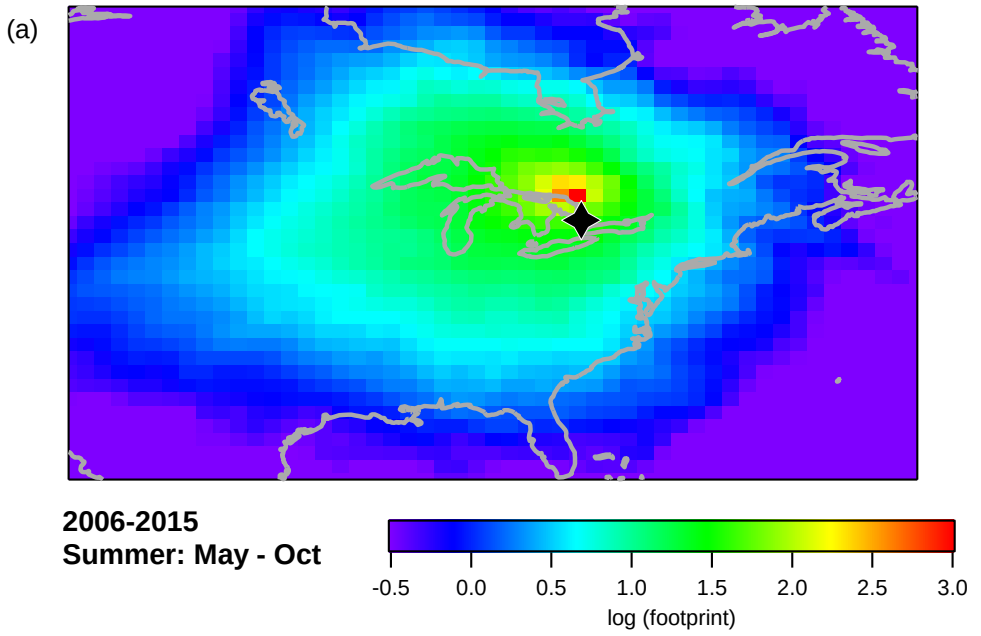

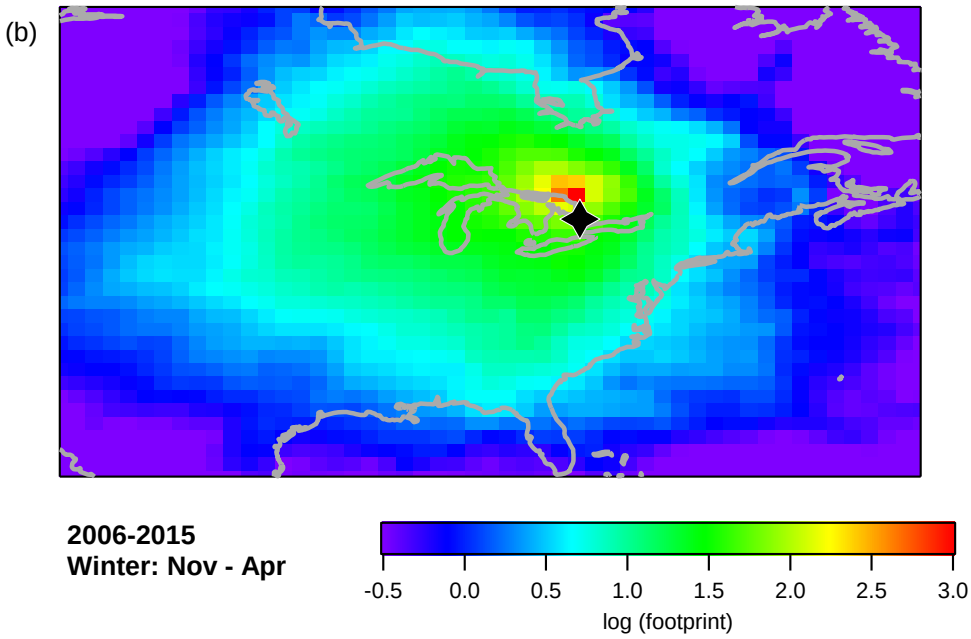

References

Beverly, R.K., Beaumont, W., Tauz, D., Ormsby, K.M., von Reden, K.F., Santos, G.M. and Southon, J.R.: The Keck Carbon Cycle AMS Laboratory, University of California, Irvine: Status report, Radiocarbon 52(2), 301-309, 2010.

Chan, T. W., Huang, L., Leaitch, W. R., Sharma, S., Brook, J. R., Slowik, J. G., Abbatt, J. P. D., Brickell, P. C., Liggio, J., Li, S. M., and Moosmüller, H.: Observations of OM/OC and specific attenuation coefficients (SAC) in ambient fine PM at a rural site in central Ontario, Canada, Atmos. Chem. Phys, 10, 2393-2411, 2010.

Chow, J. C., Watson, J. G., Pritchett, L. C., Pierson, W. R., Frazier, C. A., and Purcell, R. G.: The DRI Thermal/Optical Reflectance carbon analysis system: Description, evaluation and applications in U.S. air quality studies, Atmos. Environ., 27A, 1185-1201, 1993.

Chow, J. C., Watson, J. G., Chen, L.-W. A., Chang, M.-C. O., Robinson, N. F., Trimble, D. L., and Kohl, S. D.: The IMPROVE_A temperature protocol for thermal/optical carbon analysis: Maintaining consistency with a long-term database, J. Air Waste Manage. Assoc., 57, 1014-1023, 2007.

Ding, L., Chan, T. W., Ke, F. and Wang, D. K. W.: Characterization of chemical composition and concentration of fine particulate matter during a transit strike in Ottawa, Canada, Atmos. Environ., 89, 433-442, 2014.

Healy, R. M., Sofowote, U., Su, Y., Debosz, J., Noble, M., Jeong, C. H., Wang, J. M., Hilker, N., Evans, G. J., Doerksen, G., Jones, K., and Munoz, A.: Ambient measurements and source apportionment of fossil fuel and biomass burning black carbon in Ontario, Atmos. Environ., 161, 34-47, 2017.

Huang, L., Brook, J. R., Zhang, W., Li, S. M., Graham, L., Ernst, D., Chivulescu, A., and Lu, G.: Stable isotope measurements of carbon fractions (OC/EC) in airborne particulate: A new dimension for source characterization and apportionment, Atmos. Environ., 40, 2690-2705, 2006.

Lavoué, D., Liousse, C., Cachier, H., Stocks, B. J., and Goldammer, J. G.: Modeling of carbonaceous particles emitted by boreal and temperate wildfires at northern latitudes, J. Geophys. Res. Atmos., 105, 26871-26890, 2000.

Leaitch, W. R., MacDonald, A. M., Brickell, P. C., Liggio, J., Sjostedt, S. J., Vlasenko, A., Bottenheim, J. W., Huang, L., Li, S. M., Liu, P. S. K., Toom-Sauntry, D., Hayden, K. A., Sharma, S., Shantz, N. C., Wiebe, H. A., Zhang, W., Abbatt, J. P. D., Slowik, J. G., Chang, R. Y. W., Russell, L. M., Schwartz, R. E., Takahama, S., Jayne, J. T., Ng, N. L.: Temperature response of the submicron organic aerosol from temperate forests, Atmos. Environ., 45, 6696-6704, 2011.

Paasonen, P., Asmi, A., Petäjä, T., Kajos, M. K., Äijälä, M., Junninen, H., Holst, T., Abbatt, J. P. D., Arneth, A., Birmili, W., van der Gon, H. D., Hamed, A., Hoffer, A., Laakso, L., Laaksonen, A., Leaitch, W. R., Plass-Dülmer, C., Pryor, S. C., Räisänen, P., Swietlicki, E., Wiedensohler, A., Worsnop, D. R., Kerminen, V. M., and Kulmala, M.: Warming-induced increase in aerosol number concentration likely to moderate climate change, Nature Geoscience, 6, 438-442, 2013.

Santos, G.M., Moore, R., Southon, J., Griffin, S., Hinger, E., Zhang, D.: AMS 14C preparation at the KCCAMS/UCI Facility: status report and performance of small samples. Radiocarbon 49(2), 255-269, 2007.

Santos, G.M. and Xu, X.: Bag of Tricks: A Set of Techniques and other Resources to Help 14 C Laboratory setup, Sample Processing, and Beyond, Radiocarbon, 59(3), 785-801, 2017.

Stohl, A., Forster, C., Frank, A., Seibert, P., and Wotawa, G.: Technical note: The Lagrangian particle dispersion model FLEXPART version 6.2, Atmos. Chem. Phys, 5, 2461-2474, 2005.

Tunved, P., Hansson, H. C., Kerminen, V. M., Strom, J., Dal Maso, M., Lihavainen, H., Viisanen, Y., Aalto, P. P., Komppula, M., and Kulmala, M.: High natural aerosol loading over boreal forests, Science, 312, 261-263, 2006.